Luminescence dynamics of single self-assembled chains of Förster(FRET)-coupled CdSe nanoplatelets

Z. Ouzit[1], G. Baillard[1], J. Liu[1], B. Wagnon[2], L. Guillemeney[2], B. Abécassis[2] and L. Coolen[1,]*

[1]Sorbonne Université, CNRS, Institut de NanoSciences de Paris, INSP, F-75005 Paris, France

[2]Univ Lyon, CNRS, École Normale Supérieure de Lyon, Laboratoire de Chimie UMR 5182 46 allée d'Italie, F-69007 Lyon, France

** corresponding author: laurent.coolen@sorbonne-universite.fr*

Abstract

Self-assembled linear chains of CdSe nanoplatelets are known to exhibit highly efficient Förster resonant energy transfer (FRET) leading to fast exciton diffusion between platelets. Here, we compare the luminescence decay dynamics of single nanoplatelets, clusters of a few platelets, and self-assembled chains. As the number of stacked platelets is increased, we show that the luminescence decay becomes faster, which can be interpreted as FRET-mediated effect of quenchers: excitons may diffuse to nearby quenchers so that their decay rate is increased. On the other hand, a minor slow decay component is also observed for single platelets, corresponding to trapping-detrapping mechanisms in nearby trap states. The contribution of the slow component is enhanced for the platelet chains. This is consistent with a FRET-mediated trapping mechanism where the excitons would diffuse from platelet to platelet until they reach a trap state. Finally, we develop toy models for the FRET-mediated quenching and trapping effects on the decay curves and analyze the relevant parameters.

TOC Graphic

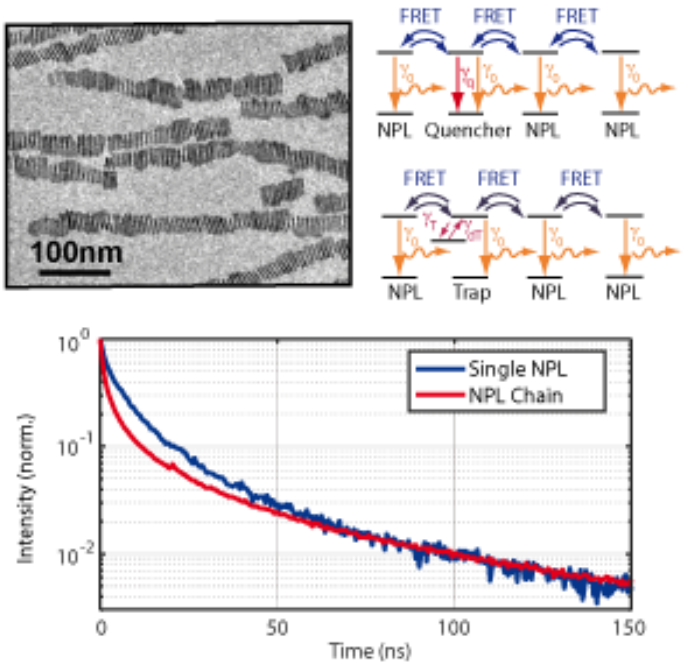

Fluorescent semiconductor nanoparticles have been under intense scrutiny during the last decades. An elaborate understanding of this class of emitters is now available and has led to various developments in opto-electronics and other fields like bio-imaging, nano-medicine and quantum optics. These studies were usually performed on isolated emitters: either on ensembles of emitters in dilute solution, or on single emitters under fluorescence microscopy. There is now an increasing interest of both the solid-states community and the nano-optics community for the collective behaviour of a large number of coupled nano-emitters**.** When a densely-packed stacking of emitters is considered, interactions between them are expected. However, experimental results are diverse and their interpretation is complex, especially because the level of disorder in stacked structures makes them difficult to model and reproduce. A fundamental understanding of the coupling between semi-conducting nanoparticles is crucial for opto-electronic applications as they often involve dense layers of semiconductor nanoparticles.

Among various coupling mechanisms, Förster-resonant energy transfer (FRET), a non-radiative dipole-dipole interaction over a typical 1-to-10-nm range, can lead to one exciton annihilation in a platelet and one exciton creation in the neighbour platelet[1]. In a sample of 2 populations of different emitters with the emission spectrum of one overlapping the absorption spectrum of the other, FRET from the former to the latter may occur (hetero-FRET). Within a *single* population of emitters without inhomogeneous broadening, if they are sufficiently close and their emission and absorption spectra overlap (low Stokes shift), excitons can be transferred between these emitters by homo-FRET. In a dense sample, a succession of homo-FRET transfers between neighbours can lead to FRET hopping and energy diffusion[2]. It has been argued that FRET can decrease the general quantum efficiency by funnelling energy to quenchers (defect particles)[3] but also that it can be beneficial for transfer to charge-collecting layers in photovoltaic cells[4] and novel FRET-enabled devices have been proposed[5,6]. FRET within a collection of nanoparticles can be manifested in its fluorescence decay curve. For instance, clusters of spherical nanocrystals have shown the presence of an additional short component, attributed to hetero-FRET between emitters of different sizes[7] or a stronger acceleration under high excitation power, explained by FRET-enhanced Auger multiexciton decay[8].

Semiconductor nanoplatelets (NPLs)[9,10], also coined colloidal quantum wells, are a system of choice for studying FRET interactions[4,11]. They display outstanding optical properties[12]: perfect monodispersity due to the thickness controlled at the atomic level; in-plane dipoles[13-15] and giant oscillator strength[10]. They have shown promising results for opto-electronics[16,17] such as light-emitting diodes[18] and very low threshold lasers[19,20]. When mixing NPLs of different thicknesses, hetero-FRET has been evidenced by a faster decay curve for the donor NPLs[21,22]. Within a single NPL population, homo-FRET should not modify the decay curve as the decay of the total population is not changed. However, increased decay rates have been reported for stacked NPLs and attributed to FRET-mediated action of a quencher platelet[3,23-26]: excitons in neighbour platelets diffuse to the quencher platelet by FRET so that a single defect will quench a large number of platelets.

Self-assembled chains of CdSe NPLs[27-29] constitute a remarkable model system to study interactions between nanoparticles. Previous research[30] has shown that energy diffusion by FRET can extend over around 90 NPLs, which would correspond to a hopping time between neighbours of the order of 1 ps, much faster than other types of nanoparticles. Because many decay mechanisms in isolated NPLs are much slower than 1 ps, FRET can lead within NPL ensembles to behaviors much different from the simple sum of isolated NPLs, as illustrated by our recent demonstration of collective blinking from a few tens of NPLs[31].

In this paper, we analyze the fluorescence decay curves of different CdSe NPL assemblies: small clusters, short chains, longer chains. As compared to single isolated NPLs, the chains display a highly non-exponential decay curve. We show that the initial decay becomes faster for stacked platelets, but

also that a slow decay component becomes more significant. Both observations are consistent with FRET-enhanced effects of quenchers and traps states. We model these effects within a framework of population equations and identify different possible regimes.

CdSe nanoplatelets were synthesized as described in former work[31] with a 1.5-nm thickness (6 Cd layers + 5 Se layers) and $(7 \pm 2) \times (20 \pm 4)$ nm² lateral dimensions as deduced from TEM images (fig. 1(a)). The absorption spectrum (fig. 1(b)) shows peaks caused by quantum confinement and the emission spectrum is a line centered at 549 nm. Due to the very monodisperse thickness of the nanoplatelets, there is no measurable dispersion of the single-NPL emission wavelength and the ensemble spectrum measured in solution is the same as the emission spectrum of single NPLs so that homo-FRET can occur[30]. The low Stokes shift ensures a good overlap between absorption and emission spectra hence efficient FRET transfer. The platelets were then assembled in solution in the presence of oleic acid and formed one-dimensional organized chains, as shown on the TEM image of figure 1(c). The length of the chains ranged from a few hundreds of nanometers to a few microns. The NPL center-to-center distance was estimated as 5.7 nm from TEM images (detailed discussion in former work[30]).

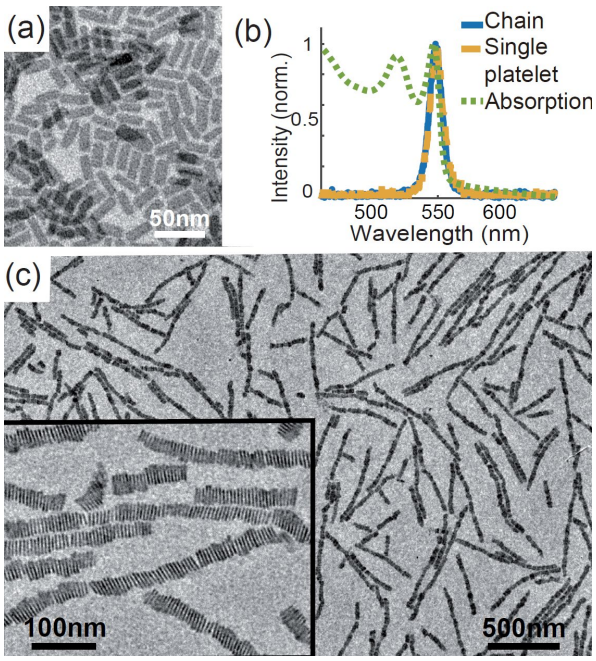

Figure 1 : (a) TEM image of single CdSe nanoplatelets. (b) Absorption spectrum (green dotted line) of a NPL solution. Photoluminescence spectra of a single NPL (yellow dashed line) and a NPL chain (blue full line) under 473 nm excitation. (c) TEM image of NPL chains.

The samples were deposited on a glass slide and observed by fluorescence microscopy with an imaging resolution (point spread function – PSF) of 190-nm radius. The emitters were excited by a 473-nm pulsed diode laser at power 5-10 nW. The fluorescence emission was detected by single-photon avalanche photodiodes (setup response function 350 ps) in Hanbury-Brown and Twiss configuration.

Two classes of samples were prepared. On the one hand, a solution of isolated platelets was deposited. We observed spots of size limited by the PSF and analyzed their emission autocorrelation

($g^{(2)}(\tau)$ function) (figs. 2(a,b)). It is known that, depending on their size, single NPLs may exhibit more or less complete antibunching[32,33]. Theoretically, in the simple case of emission originating from N identical emitters, the normalized area of the central $g^{(2)}$ peak is $= 1 - 1/N$ for perfect single-photon sources and $> 1 - 1/N$ if the emitters are not fully antibunched. Therefore, we will consider that the central $g^{(2)}$ peak area indicates a « single platelet » when it is below 0.5 (fig. 2(a)), and a « small cluster » when in the range 0.5-0.83 (fig. 2(b)). These clusters are expected, from previous studies, to be NPL stacks lying horizontally on the substrate[15]. Central peak areas above 0.83 were excluded as probably corresponding to larger clusters ($N > 6$ if the emitters are perfect single-photon sources) with unknown stacking order.

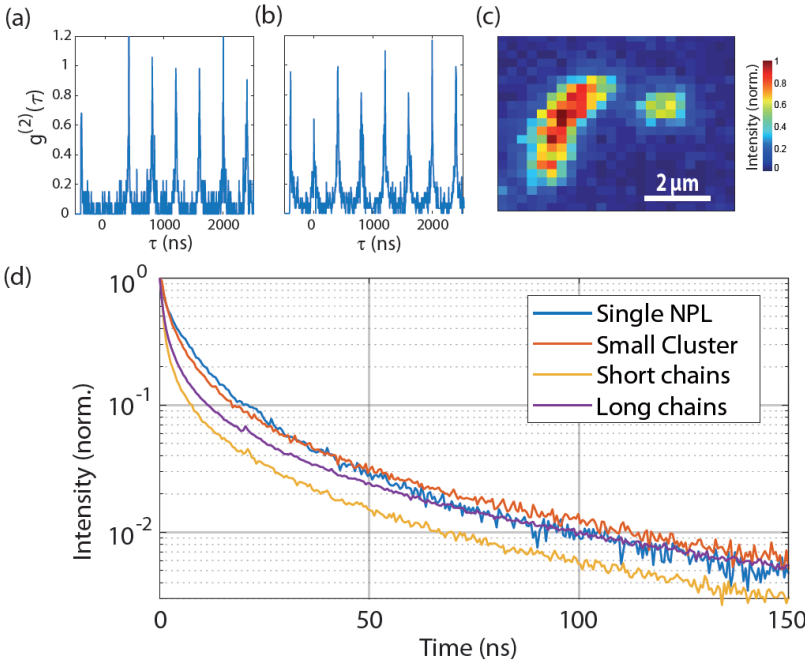

Figure 2 : Antibunching curves for (a) a single nanoplatelet and (b) a small cluster ($N \leq 6$). (c) Scanning photoluminescence image showing (left) a long chain and (right) a shorter, diffraction-limited chain. (d) Luminescence decay curves for a typical emitter of each category.

On the other hand, a solution of NPL chains was deposited. We then observed by luminescence imaging (fig. 2(c)) elongated emission threads here referred to as « long chains », and emission spots (limited by the PSF size 190 nm corresponding to $N = 35$) which we label « short chains » - although they may in fact also be large clusters rather than chains.

Figure 2(d) plots the decay curve from emitters representative of each category. The single NPL shows a rather monoexponential decay with a decay rate (6.2 ns) corresponding to the radiative decay rate. A minor component of much slower decay (61 ns) is also seen. This occurrence of « delayed emission » has been discussed for ensembles of nanoplatelets in solution[34]. It was attributed to the presence of a metastable state where one charge can become trapped and from which it is released after a long delay. The duration of this delay was found spanning a range from the ns to 10 µs[34]. For single NPLs, the same delayed emission was found with decay times of 40-100 ns[35]. Note that such times are very different from the typical time scales of blinking (from ms to mn), so that this trapping/detrapping process is not responsible for on/off blinking events. By pump-probe analysis of spin precession in CdSe/CdS core-shell NPLs[36], trapping of electrons outside the NPL was demonstrated over times up to 100 µs (while detrapping of holes was shown to occur much faster, over a few ns).

Delayed emission was then attributed to electron trapping and detrapping. Slow emission from a second redshifted level was also reported by some authors and attributed to hole trapping[35] or surface trap sites[37].

Very different decay curves are obtained for the NPL chains (fig. 2(d)). The beginning of the decay is much faster than for the single NPL. The slow component is comparable in characteristic time, but its relative contribution to the total emission is increased, for the clusters and even more for the NPL chain – as will become more apparent below.

Before discussing these observations, let us confirm them by a statistical analysis of the decays of the different emitter categories. Individual platelets show a large dispersion of decay curves, as plotted in the supporting information (S.I.) (fig. S1(a)), as well as small clusters and short chains. Quite remarkably, on the other hand, the decay curves are very similar for all different NPL chains (fig. S1(d)). From these decay curves, we extract the short decay time τ_S, defined as the time of $1/e$ decay, the long decay time τ_L, obtained by fitting the $t > 100$ ns portion of the curve with an exponential, and the contribution (fraction of photons) a_L associated to the long decay component (see Methods). The distribution of these three parameters is plotted for the different categories of emitters in figure 3 and their averages and standard deviations are summarized in table 1.

These data confirm the qualitative observations presented for the typical curves plotted on fig. 2(d). The three decay characteristics τ_S, τ_L and a_L are very dispersed for the single NPLs as a result of their inhomogeneous size dispersion, ligand coverage and presence of crystalline defect. These characteristics change gradually from single NPLs to clusters to NPL chains. The shorter component τ_S is distributed between 2 and 8 ns for the single NPL and small clusters and drops to 2 ns for the chains. The slow decay time τ_L shows a minor change from 60-80 ns for the single NPLs to mostly 80 ns for the chains. Most significantly, the slower component fraction a_L is distributed between 0 and 0.7 for the different single NPLs and undergoes a general increase to 0.4-0.5 for the NPL chains.

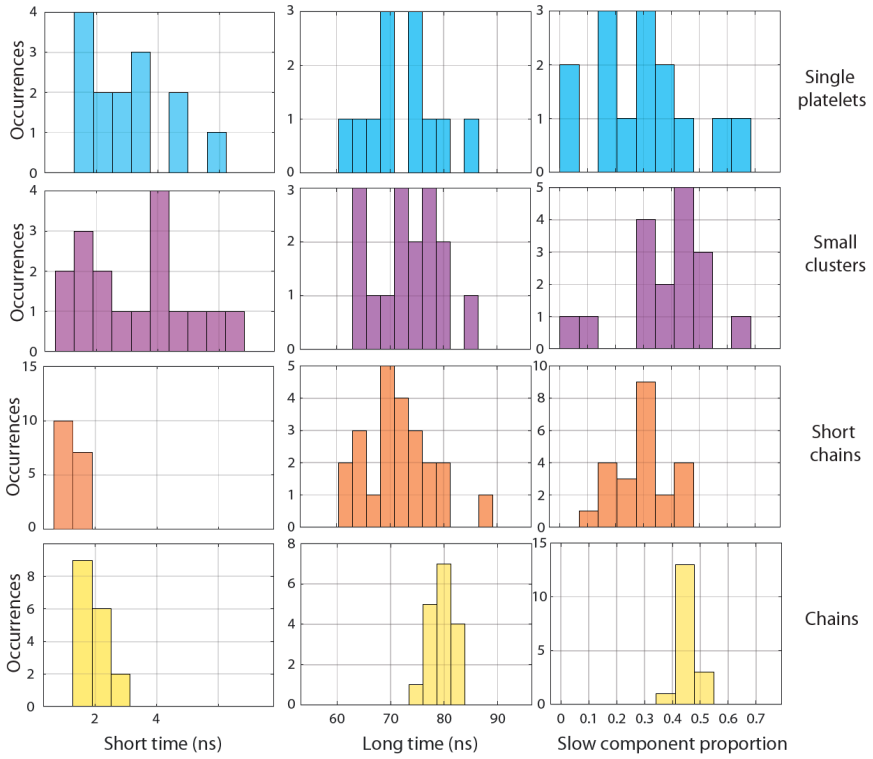

Figure 3: Distribution of the short decay time τ_S, the long decay time $\tau_L$and the fraction a_L of photons contributing to the slow decay component, for the single platelets, for the small clusters ($N \leq 6$), for the short chains ($N \leq 35$) and the long chains ($N > 35$).

	Short time τ_S	Long time τ_L	Fraction a_L
Single NPLs	3.0 ns (1.4 ns)	72 ns (7 ns)	0.29 (0.19)
Small clusters	3.3 ns (1.7 ns)	73 ns (7 ns)	0.38 (0.15)
Short chains	1.2 ns (0.3 ns)	72 ns (6 ns)	0.30 (0.10)
Long chains	2.0 ns (0.4 ns)	79 ns (2 ns)	0.45 (0.03)

Table 1: Decay parameters τ_S, $\tau_L$and a_L for the different collections of emitters considered: average values and standard deviations (standard deviations are given in parentheses).

For single NPLs, τ_S corresponds mostly to the radiative decay time. Our observed decay acceleration (decrease of τ_S) is similar to previous reports for stacked NPLs[3,23-25] and for NPL chains[26,30]. It was attributed to an increased influence of quenchers due to FRET[3]: when a given emitter presents a quenching mechanism (fast additional non-radiative decay rate), emission from nearby platelets can also be quenched if excitons in these platelets are transferred efficiently to the quencher platelet (fig. 4(a)). The general decay of a NPL ensemble can thus be accelerated by a single quencher NPL. We note that this faster decay, in our results as well as in previous papers, could also originate from differences in ligand coverage between single NPLs and stacks/chains. However, our recent observation that NPL chains blink collectively demonstrates unambiguously the presence of collective quenching by FRET transfer to a single defect[31]. Here, acceleration of the fast decay is present for all chains (short or long), but much less for the small clusters, possibly because some clusters contain no quencher.

The data in figure 3 also reveal an increase in delayed emission contribution (increase in a_L) as compared to the single NPLs. We suggest that this observation is caused by FRET diffusion as well. While the presence of a trap state near a given platelet should not influence directly the neighbor platelets, excitons created inside the neighbor platelets may diffuse and reach the trap-bearing platelet by FRET, so that a whole portion of NPL chain may be subject to delayed emission (fig. 4(c)).

In order to improve our intuition of the effect of quenchers and traps, let us model a few cases. We will describe the system as a chain of N identical emitters with radiative decay rate γ_0 and a rate of FRET transfer between neighbours γ_{tr}. Following our former experimental results[30], we will choose the numerical values $1/\gamma_0$ = 10 ns and $1/\gamma_{tr}$ = 1 ps. Each emitter will be labelled by its number s ($s = 1 \dots N$) and populated by the exciton with a probability $p_s(t)$. Initially, an exciton is present at the excited emitter s_0, thus $p_{s_0}(0) = 1$ and $p_{s \neq s_0}(0) = 0$.

First, in order to describe how FRET can shorten τ_S, we add (fig. 4(a)) a quenching mechanism of rate γ_q for one of the emitters (labelled s_q). The emitters dynamics is then governed by

$$\frac{dp_s}{dt} = -\gamma_0 p_s - 2\gamma_{tr} p_s + \gamma_{tr} p_{s-1} + \gamma_{tr} p_{s+1} \quad \text{for } s \neq s_q$$

and

$$\frac{dp_s}{dt} = -(\gamma_0 + \gamma_q) p_s - 2\gamma_{tr} p_s + \gamma_{tr} p_{s-1} + \gamma_{tr} p_{s+1} \quad \text{for } s = s_q$$

These equations were solved by diagonalizing the corresponding matrix and the luminescence decay curve was calculated as the rate of photon emission $I(t) = \gamma_0 \sum p_s(t)$ and then averaged over all excitation and quencher positions s_0 and s_q. The resulting decay curves (fig. S3) are generally mono-exponential (in agreement with plots obtained by a different method[3]), except in cases where $\gamma_q > \gamma_{tr}$ and N is large: then the curve has a less exponential shape. Let us however approximate all decays by a single exponential with a decay rate of the form $\gamma = \gamma_0 + \gamma'$. Figure 4(b) plots the additional decay rate γ' caused by the quencher, as a function of the quenching rate $\gamma_q$for different values of N. The fastest decay is obtained when the quencher rate is high and when the number of emitters is low, so that the exciton diffuses easily to the quencher. When $\gamma_q \ll \gamma_{tr}$ (left portion of fig. 4(b)), FRET is much faster than quenching so that the exciton behaves as statistically delocalized over all N emitters, of which only one is a quencher: the luminescence decay is well approximated by

$$\gamma \approx \gamma_0 + \gamma_q / N$$

When $\gamma_q \gg \gamma_{tr}$ (right portion of fig. 4(b)), on the other hand, quenching is much faster than FRET so that, when the exciton reaches the quencher, it will always be quenched. Then the limiting factor is the time necessary for the exciton to diffuse and reach the quencher. As a result, γ' is independent on γ_q and scales roughly as $1/N^2$ (inset of fig. 4(b)), consistent with a diffusion mechanism.

Quenching in semiconductor nanoplatelets is often attributed to Auger decay in charged states. Auger decay in CdSe nanoplatelets is of the order of a few tens or hundreds of ps[17,19,38,39] so that our platelets should be closer to the regime $\gamma_q \ll \gamma_{tr}$. For the NPL chains, our measured short decay may then be approximated as $1/\tau_S = \gamma_0 + \gamma_q/N$. This explains that τ_S is shorter for the chains than for the single NPLs (fig. 3).

More precisely, according to the latter equation, the fast decay time should be shorter for the chains ($\tau_S = 1/(\gamma_0 + \gamma_q/N)$) than for the single platelets *without* quencher ($\tau_S = 1/\gamma_0$), but longer than for the single platelets *with* quencher ($\tau_S = 1/(\gamma_0 + \gamma_q)$). This is not exactly verified for the short chains: most of them have shorter decay than *all* single platelets (fig. 3). However, these decays (0.5-

1 ns) are very close to the shortest decays of the single NPLs (≈ 1.5 ns) so that the difference might not be really significant. Moreover, if a single platelet has very short τ_S, its emission is strongly quenched so that it may not be observable: this may cause a truncation of the single-NPL τ_S distribution at short times. It is well-known in fact that quenching in such single nano-emitters can be much faster than 1 ns.

Eventually, even though the present model aims at understanding only qualitatively the effect of FRET-mediated quenching, let us discuss the orders of magnitude. With $N \sim 10 - 100$ and $1/\gamma_0 \sim$ 5 ns, the measured $\tau_S = 2$ ns for the chains (fig. 3) would lead to an estimate of $1/\gamma_q \sim$ 30-300 ps, which would be a reasonable order of magnitude as compared to literature values for the Auger rate.

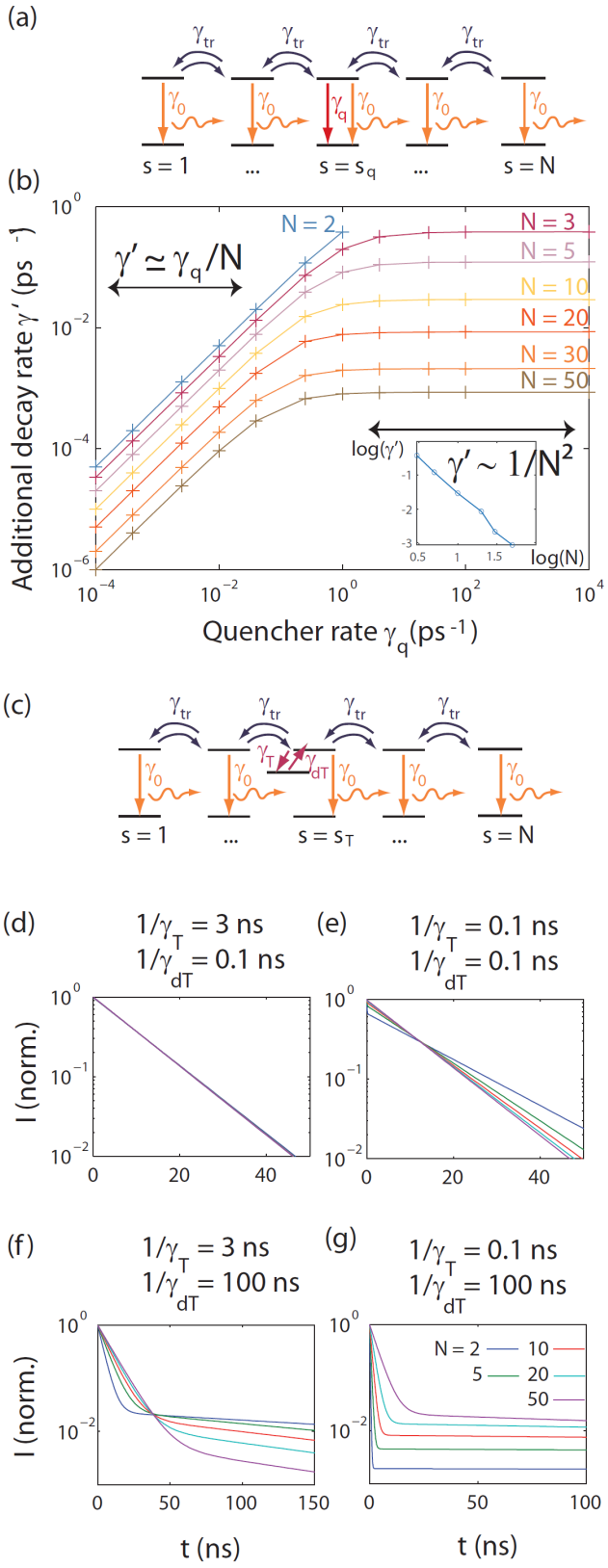

Figure 4 : (a) Model for FRET-mediated quenching: N emitters with radiative decay rate γ_0 and transfer rate γ_{tr} with an additional quenching rate γ_q for the emitter numbered $s = s_q$. (b) Additional decay rate γ' (defined in S.I.-B) due to FRET-mediated quenching, for γ_{tr} = (1 ps)$^{-1}$. (c) Model for FRET-mediated trapping: now the emitter numbered $s = s_T$ is connected to a trap state by trapping and detrapping rates γ_T and γ_{dT}. (d) to (g) Obtained decay curves for γ_0 = (10 ns)$^{-1}$, γ_{tr} = (1 ps)$^{-1}$ and various values of γ_T, γ_{dT} and N.

We now wish to account for the slow component in the experimental decay curves by introducing in the model a FRET-mediated trapping mechanism (fig. 4(c)): one of the emitters, labelled s_T, bears a trap state with respective trapping and detrapping rates γ_T and γ_{dT} . The system then obeys

$$\frac{dp_s}{dt} = -\gamma_0 p_s - 2\gamma_{tr} p_s + \gamma_{tr} p_{s-1} + \gamma_{tr} p_{s+1} \quad \text{for } s \neq s_T,$$

$$\frac{dp_s}{dt} = -(\gamma_0 + \gamma_T) p_s - 2\gamma_{tr} p_s + \gamma_{dT} p_T + \gamma_{tr} p_{s-1} + \gamma_{tr} p_{s+1} \text{ for } s = s_T$$

$$\text{and } \frac{dp_T}{dt} = -\gamma_{dT} p_T + \gamma_T p_{s_T} \quad \text{for the trap population } p_T$$

We solve this system of equations, average over all excitation and trap positions (respectively s_0 and s_T) and plot the resulting decay curves in figs. 4(d) to (g) for a few sets of parameters γ_T, γ_{dT} and N (the data for more parameter values can be found in figs. S4, S5 and S6).

In fig. 4(d), the trapping mechanism is slow (3 ns) and detrapping is fast (0.1 ns) so that the decay curve is just the single exponential of rate γ_0, with no effect of the trap.

In fig. 4(e), trapping is much faster (0.1 ns) but detrapping is also very fast ($1/\gamma_{dT}$ = 0.1 ns), so that the decay remains close to the γ_0 exponential, with only a minor fast component added in the lower-N cases.

In contrast, the effect of the trap is clear in figs. 4(f) and (g) as a result of the much slower detrapping (100 ns). The decay curve then consists in a bi-exponential. The fast component corresponds to the quenching of luminescence by trapping of the exciton. It becomes faster as γ_T is increased and slower as N is increased – because it takes more time to reach the trap if the chain is longer. The slow component corresponds to the delayed emission which occurs after the exciton exits the trap. We note that it becomes slower for lower N and higher γ_T, because then the probability for retrapping increases so that the emission delaying is enhanced. For instance, with $1/\gamma_T$ = 1 ns and $1/\gamma_{dT}$ = 100 ns, we find a slow decay time of 305 ns for N = 5 and 120 ns for N = 50 (see fig. S5). This decrease with N is actually not in agreement with the experiment, which finds a rather constant τ_L, (and even slightly longer for the long chains: 10 % increase). This illustrates the limitations of our simplified model of FRET-mediated trapping. For instance, it includes only one quencher or trap within the chain, while the number of quenchers or traps would probably increase with N.

Simple analytical expressions can be obtained if we assume the exciton diffuses very quickly over the whole chain: $\gamma_{tr}/N^2 \gg \gamma_0, \gamma_T, \gamma_{dT}$ (the obtained conclusions are, with the parameters considered in figs. 4, S4, S5 and S6, valid quantitatively for the lower Ns and qualitatively for the higher Ns). Then, one can assume that the exciton is statistically distributed equally over all platelets and treat the problem as a trapping/detrapping between the chain and the trap (see full treatment in S.I. section C). Eventually, for an efficient trap (overall trapping rate γ_T/N much faster than γ_0 and γ_{dT}), we find that the decay curve will present a fast component $\approx \gamma_T/N + \gamma_0$ and a slow component $\approx \gamma_0 \gamma_{dT} N/\gamma_T$, which agrees with the qualitative observations of figs. 4(f) and (g).

The fast component is the same as in the quencher model (fig. 4(a)): the effect of the trap is the same as the effect of a quencher in terms of acceleration of the γ_0 decay rate. Like before, we may estimate $1/\gamma_T \sim$ 30-300 ps for our experimental situation, although the validity of the model is most likely just qualitative. However, because the trap can release its exciton later (while the quencher can only relax it), it also introduces a slow delayed-emission component. With the experimental values $1/\gamma_0 \sim$ 5 ns, $\tau_L \sim$ 80 ns and $N/\gamma_T \sim$ 3 ns, our simple model yields an order of magnitude of $1/\gamma_{dT} \sim$ 50 ns.

To conclude, we have measured the luminescence decay curves of single nanoplatelets and stacks of different numbers of platelets (small clusters, shorter and longer chains). We observed, for the stacked platelets, an acceleration of the shorter (main) decay component, and an enhancement of the slower (delayed-emission) contribution. The acceleration can be attributed to FRET-mediated effect of quencher platelets, in agreement with our previous observation of FRET-mediated collective blinking. The enhancement of the slower component would be consistent with a FRET-mediated trapping mechanism, where an exciton in a given platelet might diffuse by FRET until it reaches a trap. We have presented simple toy models which adequately describe the physical mechanisms of FRET-mediated quenching and trapping. Within these models, our experimental data would be consistent with reasonable time orders of magnitude of 30-300 ps for quenching (or trapping) and 50 ns for detrapping.

Methods

- Fluorescence microscopy

We performed optical measurements using a home-built inverted fluorescence microscope equipped with a laser scanning system. We used an immersion objective (Olympus apochromat 100x, 1.4 N.A.), mounted on a piezo-electric stage, to both excite the emitters by focusing a 473 nm diode laser beam (PDL 800-D PicoQuant, 70 ps pulses, 2.5 MHz rate) and collect their emission. The scattered excitation light was filtered by a set of filters, and only the 549 nm fluorescence is measured. The fluorescence signal then went through a polarizing beam splitter and each path led to an avalanche photodiode (PerkinElmer SPCM) of resolution 200 ps.

During all measurements, the laser excitation power ranged typically from 5 to 10 nW within the linear excitation regime of the emitters.

To prepare the samples for optical study, the solution of single NPLs was diluted (between 1000× and 10000x) in hexane and spin-coated on a glass slide at 4000 rpm for 40 s to get well-separated single emitters. The chain samples were prepared differently to maintain their integrity. The glass slide was first rinsed with hexane. Then, the solution of chains was spin-coated along with pure hexane in order to dilute smoothly the solution at 4000 rpm for 40 s. The samples then presented droplets on the glass surface where preserved chains were imprisoned. The glass slide was put in vacuum in order to evaporate the droplets.

- Decay curves

The decay curves were obtained by exciting a single emitter with the pulsed laser (70 ps pulse width with 2.5 MHz rate) and detecting the fluorescence with the single-photon counting photodiodes of resolution 200 ps combined with PicoHarp acquisition card. The total system response function has a characteristic time of around 350 ps (fig. S2). The fast component decay time was estimated as the time for $1/e$ decay. The slow component decay time was found by fitting the $t > 100$ ns portion of the curve by an exponential $A_L e^{-t/\tau_L}$ (for emitters that actually present a significant component at long times). The contribution of the slow component was obtained by dividing the number of photons associated to this fitted slow component by the total number of photons (obtained by integrating the raw decay curve):

$$a_L = \frac{A_L \times \tau_L}{\int I(t)dt}$$

- Photon correlation function measurement

We measured the photon-correlation function of isolated emitters under Hanbury-Brown and Twiss configuration with a polarizing beam splitter cube (50:50) to separate the emitted photon flux into reflection/transmission paths to be detected by the two avalanche photodiodes.

Supporting information: A – Experimental decay curves. B – First model: FRET-mediated quenching (fig. 4(a)). C – Second model: FRET-mediated trapping (fig. 4(c)).

Acknowledgements

The present work was funded by the French Agence Nationale de la Recherche (project Foenics ANR-20-CE30-0012). This article is part of a project that has received funding from the European Research Council (ERC) under the European Union's Horizon 2020 research and innovation programme (Grant agreement No. 865995).

References

(1) G. A. Jones and D. S. Bradshaw, Resonance energy transfer: from fundamental theory to recent applications, *Front. Phys*. **2019,** *7*.

(2) N. Kholmicheva, P. Moroz, H. Eckard, G. Jensen and M. Zamkov, Energy transfer in quantum dot solids, *ACS Energy Lett.* **2017**, *2* (1), 154-160.

(3) B. Guzelturk, O. Erdem, M. Olutas, Y. Kelestemur and H. V. Demir, Stacking in colloidal nanoplatelets: tuning excitonic properties, *ACS Nano* **2014**, *8* (12), 12524-12533.

(4) I. Moreels, Energy transfer is speeded up in 2D, *Nature materials* **2015**, *14* (5), 464-465.

(5) B. Guzelturk and H. V. Demir, Near-field energy transfer using nanoemitters for optoelectronics, *Adv. Funct. Mater.* **2016**, *26* (45), 8158-8177.

(6) N. Hasanov, V. K. Sharma, P. L. Hernandez Martinez, S. T. Tan and H. V. Demir, Critical role of Cdse nanoplatelets in color-converting CdSe/ZnS nanocrystals for InGaN/GaN light-emitting diodes, *Optics Lett.* **2016**, *41* (12), 2883-2886.

(7) D. P. Shepherd, K. J. Whitcomb, K. K. Milligan, P. M. Goodwin, M. P. Gelfand and A. Van Orden, Fluorescence intermittency and energy transfer small clusters of semiconductor quantum dots, *J. Phys. Chem. C* **2010**, *114* (35), 14831-14837.

(8) M. Rafipoor, R. Koll, J.-P. Merkl, L. S. Fruhner, H. Weller and H. Lange, Resonant energy transfer can trigger multiexciton recombination in dense quantum dot ensembles, *Small* **2019**, *15* (5), 1803798.

(9) S. Ithurria and B. Dubertret, Quasi 2D colloidal CdSe platelets with thicknesses controlled at the atomic level, *J. Am. Chem. Soc.* **2008**, *130* (49), 16504-16505.

(10) S. Ithurria, M. D. Tessier, B. Mahler, R. P. S. M. Lobo, B. Dubertret and Al. L. Efros, Colloidal nanoplatelets with two-dimensional electronic structures, *Nature Materials* **2011,** *10* (12), 936-941.

(11) A. Dutta, A. Medda and A. Patra, Recent advances and perspectives on colloidal semiconductor nanoplatelets for optoelectronic applications, *J. Phys. Chem. C* **2021,** *125* (1), 20-30.

(12) J. Yu and R. Chen, Optical properties and applications of two-dimensional CdSe nanoplatelets, *InfoMat*. **2020**, *2* (5), 905-927.

(13) F. Feng, L. T. NGuyen, M. Nasilowski, B. Nadal, B. Dubertret, L. Coolen and A. Maître, Consequence of shape elongation on emission asymmetry for colloidal CdSe/CdS nanoplatelets, *Nano Research* **2018,** *11* (7) , 3593-3602.

(14) F. Feng, L. T. NGuyen, M. Nasilowski, B. Nadal, B. Dubertret, A. Maître and L. Coolen, Probing the fluorescence dipoles of single cubic CdSe/CdS nanoplatelets with vertical or horizontal orientations, *ACS Photonics* **2018,** *5* (5), 1994-1999.

(15) J. Liu, L. Guillemeney, A. Choux, A. Maître, B. Abécassis and L. Coolen, Fourier imaging of single self-assembled CdSe nanoplatelet chains and clusters reveals out-of-plane dipole contribution, *ACS Photonics* **2020,** *7* (10), 2825-2833.

(16) B. T. Diroll, Colloidal quantum wells for optoelectronic devices, *J. Mater. Chem. C* **2020**, *8* (31), 10628-10640.

(17) M. Pelton, Carrier dynamics, optical gain, and lasing with colloidal quantum wells, J. Phys. Chem. C **2018**, *122* (20), 10659-10674.

(18) P. Xiao, J. Huang, D. Yan, D. Luo, J. Yuan, B. Liu and D. Liang, Emergence of nanoplatelet light-emitting diodes, *Materials* **2018**, *11* (8), 1376.

(19) C. She, I. Fedin, D. S. Dolzhnikov, A. Demortière, R. D. Schaller, M. Pelton and D. V. Talapin, Low-threshold stimulated emission using colloidal quantum wells, *Nano Lett*. **2014**, *14* (5), 2772-2777.

(20) J. Q. Grim, S. Christodoulou, F. Di Stasio, R. Krahne, R. Cingolani, L. Manna and I. Moreels, Continuous-wave biexciton lasing at room temperature using solution-processed quantum wells, *Nature Nanotech.* **2014,** *9* (11), 891-895.

(21) C. E. Rowland, I. Fedin, H. Zhang, S. K. Gray, A. O. Govorov, D. V. Talapin and R. D. Schaller, Picosecond energy transfer and multiexciton transfer outpaces Auger recombination in binary CdSe nanoplatelet solids, *Nature Materials* **2015**, *14* (5), 484-489.

(22) B. Guzelturk, M. Olutas, S. Delikanli, Y. Kelestemur, O. Erdem and H. V. Demir, Nonradiative energy transfer in colloidal CdSe nanoplatelet films, *Nanoscale* **2015**, *7*, 2545-2551.

(23) A. Antanovich, A. Prudnikau, A. Matsukovich, A. Achtstein and M. Artemyev, Self-assembly of CdSe nanoplatelets into stacks of controlled size induced by ligand exchange, *J. Phys. Chem. C* **2016***, 120* (10), 5764-5775.

(24) Y. Gao, M. C. Weidman and W. A. Tisdale, CdSe nanoplatelet films with controlled orientation of their transition dipole moment, *Nano Lett.* **2017***, 17* (6), 3837-3843.

(25) Z. Wen, P. Liu, J. Ma, S. Jia, X. Xiao, S. Ding, H. Tang, H. Yang, C. Zhang, X. Qu, B. Xu, K. Wang, K. L. Teo and X. W. Sun, High-performance ultrapure green CdSe/CdS core/crown nanoplatelet light-emitting diodes by suppressing nonradiative energy transfer, *Adv. Electron. Mater.* **2021***, 7*, 2000965.

(26) W. D. Kim, D.-E. Yoon, D. Kim, S. Koh, W. K. Bae, W.-S. Chae and D. C. Lee, Stacking of colloidal CdSe nanoplatelets into twisted ribbon superstructures, *J. Phys. Chem C* **2019***, 123* (14), 9445-9453.

(27) B. Abécassis, M. D. Tessier, P. Davidson and B. Dubertret, Self-assembly of CdSe nanoplatelets into giant micrometer-scale needles emitting polarized light, *Nano Lett.* **2014***, 14* (2), 710-715.

(28) S. Jana, T. N. T. Phan, C. Bouet, M. D. Tessier, P. Davidson, B. Dubertret and B. Abécassis, Stacking and colloidal stability of CdSe nanoplatelets, *Langmuir* **2015**, *31* (38), 10532-10539.

(29) B. Abécassis, Three-dimensional self-assembly of semiconducting colloidal nanocrystals: from fundamental forces to collective optical properties, *Chem Phys Chem* **2016**, *17* (5), 618-631.

(30) J. Liu, L. Guillemeney, B. Abécassis and L. Coolen, Long range energy transfer in self-assembled stacks of semiconducting nanoplatelets, *Nano Lett.* **2016**, *20* (5), 3465-3470.

(31) Z. Ouzit, J. Liu, J. Pintor, B. Wagnon, L. Guillemeney, B. Abécassis and L. Coolen, FRET-mediated collective blinking of self-assembled stacks of CdSe semiconducting nanoplatelets, *ACS Photonics* **2023**, *10* (2), 421-429.

(32) E. Benjamin, V. J. Yallapragada, D. Amgar, G. Yang, R. Tenne and D. Oron, Temperature dependence of excitonic and biexcitonic decay rates in colloidal nanoplatelets by time-gated photon correlation, *J. Phys. Chem. Lett.* **2020**, *11* (16), 6513-6518.

(33) X. Ma, B. T. Diroll, W. Cho, I. Fedin, R. D. Schaller, D. V. Talapin, S. K. Gray, G. P. Wiederrecht and D. J. Gosztola, Size-dependent biexciton quantum yields and carrier dynamics of quasi-two-dimensional core/shell nanoplatelets, *ACS Nano* **2017***, 11* (9), 9119-9127.

(34) F. Rabouw, J. C. van der Bok, P. Spinicelli, B. Mahler, M. Nasilowski, S. Pedetti, B. Dubertret and D. Vanmaekelbergh, Temporary charge carrier separation dominates the photoluminescence decay dynamics of colloidal CdSe nanoplatelets, *Nano Lett.* **2016**, *16* (3), 2047-2059.

(35) S. O. M. Hinterding, B. B. V. Salzmann, S. J. W. Vong, D. Vanmaekelbergh, B. M. Weckhuysen, E. M. Hutter and F. T. Rabouw, Single trap states in single CdSe nanoplatelets, *ACS Nano* **2021**, *15* (4), 7216-7225.

(36) D. Feng, D. R. Yakovlev, B. Dubertret and M. Bayer, Charge separation dynamics in CdSe/CdS core/shell nanoplatelets addressed by coherent electron spin precession, *ACS Nano* **2020**, *14* (6), 7237-7244.

(37) S. Delikanli, G. Yu, A. Yeltik, S. Bose, T. Erdem, J. Yu, O. Erdem, M. Sharma, V. K. Sharma, U. Quliyeva, S. Shendre, C. Dang, D. H. Zhang, T. C. Sum, W. Fan and H. V. Demir, Ultrathin highly luminescent two-monolayer colloidal CdSe nanoplatelets, *Adv. Funct. Mater.* **2019**, *29* (35), 1901028.

(38) Q. Li and T. Lian, Area- and thickness-dependent biexciton Auger recombination in colloidal CdSe nanoplatelets: breaking the “universal volume scaling law”, *Nano Lett.* **2017**, *17* (5), 3152-3158.

(39) J. P. Philbin, A. Brumberg, B. T. Diroll, W. Cho, D. V. Talapin, R. D. Schaller and E. Rabani, Area and thickness dependence of Auger recombination in nanoplatelets, *J. Chem. Phys.* **2020**, *153* (5), 054104.